

# Performance Analysis of Periodic Gaits in Multi-Legged Locomotion

Manuel F. Silva, J. A. Tenreiro Machado

Dept. of Electrical Engineering  
Institute of Engineering of Porto  
Rua Dr. Antonio Bernardino de Almeida,  
4200-072 Porto, Portugal  
Email: {mfs,jtm}@dee.isep.ipp.pt

António M. Lopes

Dept. of Mechanical Engineering  
Faculty of Engineering of Porto  
Rua Dr. Roberto Frias,  
4200-465 Porto, Portugal  
Email: aml@fe.up.pt

## Abstract

*This paper presents the kinematic study of periodic gaits for multi-legged locomotion systems. The main purpose is to determine the kinematic characteristics and the system performance during walking. For that objective the prescribed motion of the robot is completely characterized in terms of several locomotion variables such as gait, duty factor, body height, step length, stroke pitch, maximum foot clearance, link lengths and cycle time. In this work, we formulate two indices to quantitatively measure the performance of the walking robot namely the perturbation analysis and the locomobility measure. A set of experiments reveal the influence of the locomotion variables in the proposed indices.*

## 1. Introduction

Walking machines allow locomotion in terrain inaccessible to other type of vehicles since they do not need a continuous support surface. On the other hand, the requirements for leg coordination and control impose difficulties beyond those encountered in wheeled robots [1,2]. Gait selection is a research area, requiring an appreciable modeling effort for improvement of mobility with legs in unstructured terrain [3,4]. Previous studies focused in the structure and selection of locomotion modes. Nevertheless, there are different optimization criteria such as energy efficiency, stability, velocity, comfort, mobility and environmental impact [5,6,7]. With these facts in mind, a simulation model for multi-leg locomotion systems was developed, for several periodic gaits. Two kinematic indices were established to measure, the sensitivity of the foot cartesian trajectories to disturbances in the joints variables and the mechanical capability to implement the desired foot and body trajectories.

The foot and body trajectories are analyzed in what concerns its variation with the gait, duty factor, step length, maximum foot clearance and body height. Several

simulation experiments reveal the system configuration and the type of the movements that leads to a better mechanical implementation for a given locomotion mode, from the viewpoint of the indices.

The remainder of this paper is organized as follows. Section two introduces the kinematic model for a multi-legged robot and the motion planning algorithms. Sections three and four formulate the optimizing kinematic indices and develop a set of experiments that establish the influence of the mechanical parameters in the periodic gaits, respectively. Finally, section five outlines the main conclusions.

## 2. A model for multi-legged locomotion

In our work we consider a longitudinal walking system with  $2n$  legs ( $n \geq 2$ ), with the legs equally distributed along both sides of the robot body having, each one, two rotational joints. The even legs are on the left side of the robot and the odd legs on the right side. All legs are numbered from the front of the robot to the back.

Motion is described by means of a coordinate system associated to each leg (Fig. 1). Defining the leg lengths  $L_1$  and  $L_2$ , the cycle time  $T$ , the duty factor  $\beta$ , the transference time  $t_T = (1-\beta)T$ , the support time  $t_S = \beta T$ , the step length  $L_S$ , the stroke pitch  $S_P$ , the body height  $H_B$  and maximum foot clearance  $F_C$ , we consider a periodic trajectory for each foot, maintaining a constant body velocity  $V_F = L_S/T$ .

A fundamental problem in robotics is to determine the trajectories that allow the robot to walk more skillfully. In this work, the motion planning is accomplished by prescribing the Cartesian trajectories of the body and the feet. During the experiments, we examine the role of the walking gait versus  $\beta$ ,  $L_S$ ,  $H_B$  and  $F_C$ .

The algorithm for the forward motion planning accepts the body and feet trajectories in  $\{x, y\}$  as inputs and, by means of an inverse kinematics algorithm, generates the related joint trajectories, selecting the solution corresponding to a forward knee.

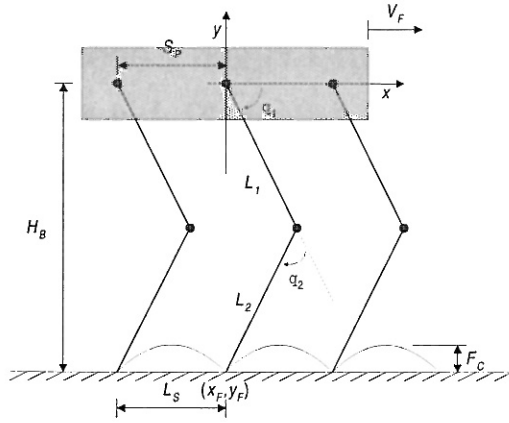


Fig. 1. Coordinate system and variables that characterize the motion trajectories of the multi-legged robot.

The body of the robot, and by consequence the leg hips are assumed to have a horizontal movement with a constant forward speed  $V_F$ . Therefore the  $\{x, y\}$  coordinates of the hip of the legs are given by (for leg  $i$ ):

$$x_{hi}(t) = V_F \cdot t \quad (1a)$$

$$y_{hi}(t) = H_B \quad (1b)$$

For a particular gait and duty factor  $\beta$  it is possible to calculate [1] for leg  $i$  the corresponding phase  $\phi_i$ , and the time instant each leg leaves and returns to contact with the ground. From these results, and knowing  $T$ ,  $\beta$  and  $t_s$ , the  $\{x, y\}$  trajectory of the tip of the foot must be completed during  $t_T$ .

For each cycle the  $\{x, y\}$  trajectory of the tip of the swing leg is computed through a cycloid function given by (considering that the transfer phase starts at  $t = 0$  sec for leg 1), with  $f = 1/T$ :

- during the transfer phase:

$$x_{F1}(t) = V_F \left[ t - \frac{1}{2\pi f} \sin(2\pi f t) \right] \quad (2a)$$

$$y_{F1}(t) = \frac{F_C}{2} [1 - \cos(2\pi f t)] \quad (2b)$$

- during the stance phase:

$$x_{F1}(t) = V_F \left[ T - \frac{1}{2\pi f} \sin(2\pi f T) \right] = V_F T \quad (3a)$$

$$y_{F1}(t) = 0 \quad (3b)$$

Based on this data, the trajectory generator is responsible for producing a motion that synchronises and co-ordinates the legs.

In order to avoid the impact and friction effects we impose null velocities of the feet in the instants of landing and taking off, assuring also the velocity continuity. These joint trajectories can also be accomplished either with a step or a polynomial acceleration time profile.

### 3. Measures for performance evaluation

In this section it is analysed the robot kinematic walking. In mathematical terms, we provide two global measures of the overall dexterity of the mechanism in an average sense [8]. The aim is to verify whether a correlation between different viewpoints can be found in walking.

#### 3.1. Perturbation Analysis

The essence of locomotion is to move smoothly the section of the body from one place to another with some restrictions in terms of execution time.

In many practical cases the robotic system is “noisy”, that is, has internal or external disturbing forces. As such, an approach called “perturbation analysis” was implemented to determine how the robot model stands with trajectory variations [8]. First, the joint trajectories are computed by the inverse kinematics algorithm. Afterwards, the angular acceleration vectors are ‘corrupted’ by additive noise. For simplicity reasons, it is used a uniform distribution, with zero mean, added to the acceleration signal. As result, the joint trajectories of the legs (and the cartesian trajectories of the feet, considering that the hip follows the right trajectory) suffer some distortion and can only approximate the desired one. By regarding the forward kinematics of the mechanism, we determine two indices based on the statistical average of the mean-square-error:

$$\xi_{\dot{x}} = \frac{1}{N_S} \sum_{i=1}^{N_S} \sqrt{\frac{1}{T} \int_0^T [\dot{x}_F^r(t) - \dot{x}_F^d(t)]^2 dt} \quad (4a)$$

$$\xi_{\dot{y}} = \frac{1}{N_S} \sum_{i=1}^{N_S} \sqrt{\frac{1}{T} \int_0^T [\dot{y}_F^r(t) - \dot{y}_F^d(t)]^2 dt} \quad (4b)$$

where  $N_S$  is the total number of steps for averaging purposes,  $\dot{x}_F^r$  and  $\dot{x}_F^d$  are the  $i$ th samples of the real and desired horizontal velocities at the foot section, respectively, and  $\dot{y}_F^r$  and  $\dot{y}_F^d$  are the  $i$ th samples of the real and desired vertical velocities at the foot. The stochastic perturbation penalises the system’s performance and we shall be concerned with minimising both indices  $\xi_{\dot{x}}$  and  $\xi_{\dot{y}}$ .

### 3.2. Locomobility Measure

The motivation for the development of the locomobility index is to apply the concepts of arm manipulability to multi-legged walking. This performance measure can be expressed through the Jacobian matrix. In our case, the global indices are obtained by averaging the distance among the center of the ellipsoids and its intersections with the desired trajectories either of the foot ( $L_F$ ) or of the body ( $L_B$ ), over a complete cycle  $T$  [8]:

$$L_F = \frac{1}{T} \int_0^T E_F(t) dt \quad (5a)$$

$$L_B = \frac{1}{T} \int_0^T E_B(t) dt \quad (5b)$$

In this perspective, the most suitable trajectory is the one that maximises  $L_F$  and  $L_B$ .

## 4. Simulation results

In this section we present a set of experiments to estimate the influence of several parameters during periodic gaits and to compare the performance measures. To evaluate the system's operating features, the simulations are carried out considering a cycle time  $T = 1$  sec,  $L_1 = L_2 = 1$  m and  $S_p = 1$  m.

Gaits describe discontinuous sequences of collective leg movements, alternating between transfer and support phases and, in the simulations, we consider the Wave, Equal Phase Half Cycle, Equal Phase Full Cycle, Backward Wave and Backward Equal Phase Half Cycle gaits {*WG, EPHC, EPFC, BW, BEPHC*} [1,9].

To illustrate the use of the preceding concepts, the multi-legged locomotion was simulated, as shown in Fig. 2.

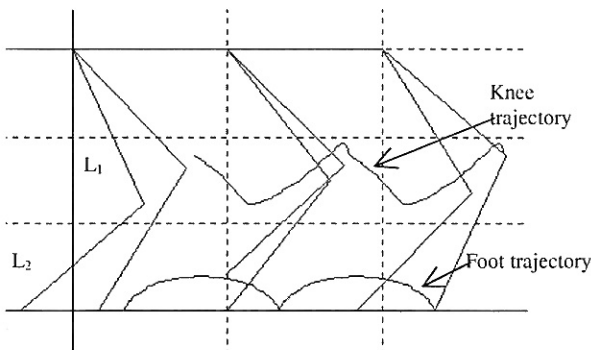


Fig. 2. Trajectories of the body, one foot and one knee of an hexapod walking robot for  $\beta = 2/3$ .

### 4.1. Duty Factor vs Body Height

For the *WG*, the perturbation analysis reveals that the higher the value of  $\beta$ , the higher are  $\xi_{\dot{x}}$  and  $\xi_{\dot{y}}$ , as can be seen in Figures 3 and 4. Moreover, this sensitivity is larger the higher the  $\beta$ .

From Figures 5 and 6 it can be seen that the locomobility indices of the foot  $L_F$  and body  $L_B$  increase slightly with  $\beta$ , but increase 'sharply' with  $H_B$ , except for high values of this parameter. Similar plots are obtained for other periodic gaits.

### 4.2. Duty Factor vs Step Length

Based on the perturbation analysis (Figures 7-8), we conclude that the indices  $\xi_{\dot{x}}$  and  $\xi_{\dot{y}}$  increase slightly with  $L_S$  and  $\beta$ . This effect is higher for values of  $\beta$  above 90%.

In what concerns the locomobility measures, Figures 9 and 10 show that  $L_S$  influences strongly  $L_F$  and  $L_B$  while the variation with  $\beta$  is weaker, except in cases of high values of  $\beta$ , where it occurs a degradation of the indices. These figures demonstrate that while  $L_B$  remains almost invariant,  $L_F$  presents a maximum for  $L_S \approx 1$  m.

### 4.3. Body Height vs Step Length

In this sub-section we show the results for both types of indices. Figures 11 and 12 reveal that  $\xi_{\dot{x}}$  and  $\xi_{\dot{y}}$  are almost insensitive to variations of  $H_B$  or  $L_S$ .

On the other hand, Figures 13 and 14 demonstrate that there is a strong influence of  $L_F$  and  $L_B$  with  $H_B$  and  $L_S$ . We see that  $L_F$  has a maximum in the middle range of  $H_B$  while  $L_B$  increases monotonically with  $H_B$ . In both cases  $L_F$  and  $L_B$  decrease slightly with  $L_S$ .

From these figures we can conclude that the robot should walk with the body in a relative high position, except in case of a high  $\beta$ .

### 4.4. Foot Clearance

From the locomobility analysis, we conclude that the type of plots do not change significantly with the robot foot clearance, but the values of  $L_F$  tend to be higher around  $F_C = 0.01$  m. As an example, we present on Figures 15 and 16 plots of  $L_F$  for  $F_C = 0.01$  m and  $F_C = 0.5$  m, respectively. Comparing Figures 15 and 16 with Figure 5, we conclude that the plots present approximately the same shape, showing that the influence of the different parameters is similar for different foot clearances. Nevertheless, the best value of  $F_C$  is around  $F_C = 0.01$  m.

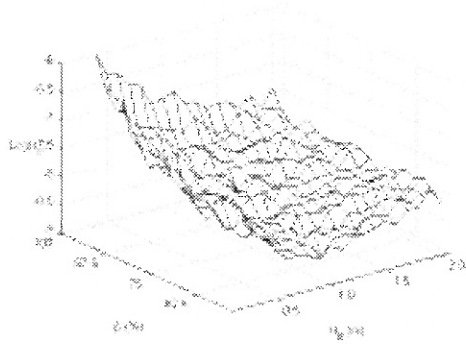


Fig. 3. Plot of  $\xi_x$  vs.  $(\beta, H_B)$  for  $F_C = 0.2$  m,  $L_S = 1$  m, WG.

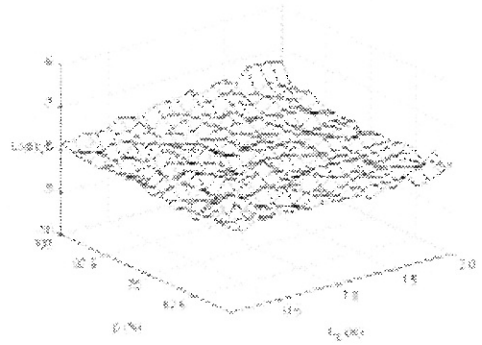


Fig. 7. Plot of  $\xi_x$  vs.  $(\beta, L_S)$  for  $F_C = 0.2$  m,  $H_B = 1.6$  m, WG.

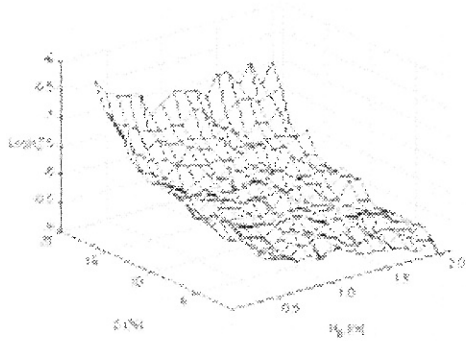


Fig. 4. Plot of  $\xi_y$  vs.  $(\beta, H_B)$  for  $F_C = 0.2$  m,  $L_S = 1$  m, WG.

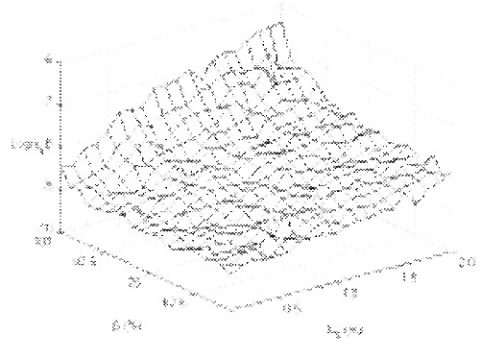


Fig. 8. Plot of  $\xi_y$  vs.  $(\beta, L_S)$  for  $F_C = 0.2$  m,  $H_B = 1.6$  m, WG.

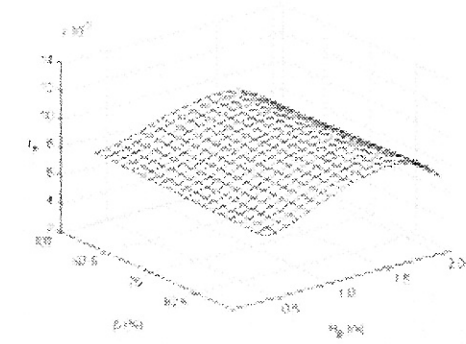


Fig. 5. Plot of  $L_F$  vs.  $(\beta, H_B)$  for  $F_C = 0.2$  m,  $L_S = 1$  m, WG.

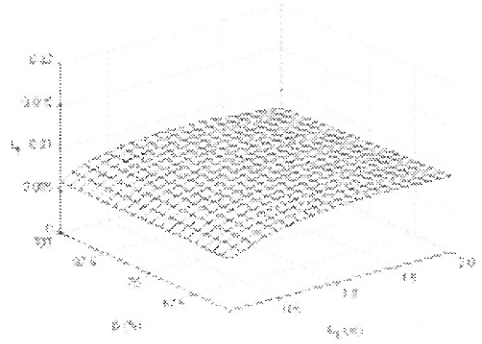


Fig. 9. Plot of  $L_F$  vs.  $(\beta, L_S)$  for  $F_C = 0.2$  m,  $H_B = 1.6$  m, WG.

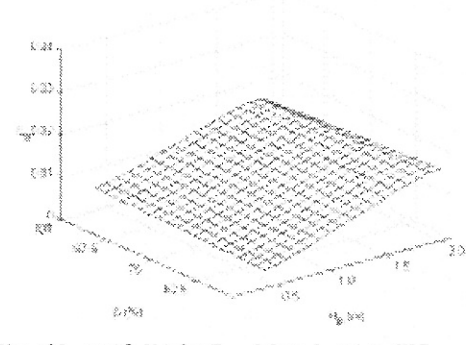


Fig. 6. Plot of  $L_B$  vs.  $(\beta, H_B)$  for  $F_C = 0.2$  m,  $L_S = 1$  m, WG.

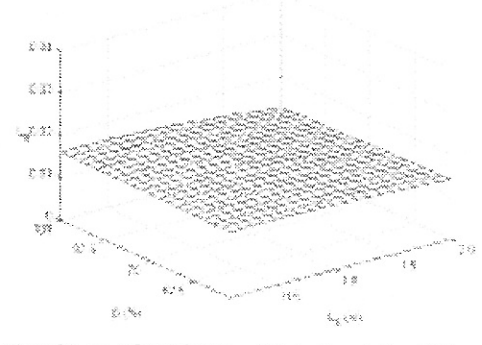


Fig. 10. Plot of  $L_B$  vs.  $(\beta, L_S)$  for  $F_C = 0.2$  m,  $H_B = 1.6$  m, WG.

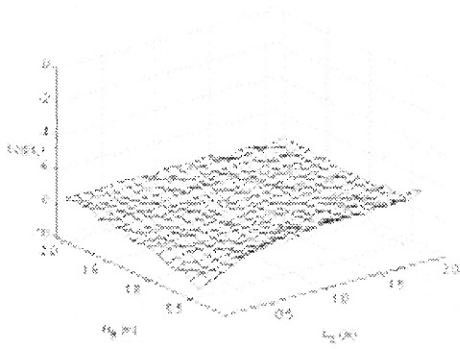


Fig. 11. Plot of  $\xi_x$  vs.  $(H_B, L_S)$  for  $F_C = 0.2$  m,  $\beta = 50\%$ , WG.

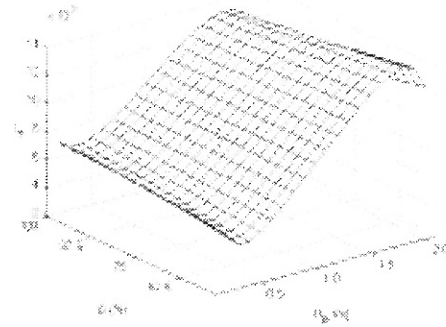


Fig. 15. Plot of  $L_F$  vs.  $(\beta, H_B)$  for  $F_C = 0.01$  m,  $L_S = 1$  m, WG.

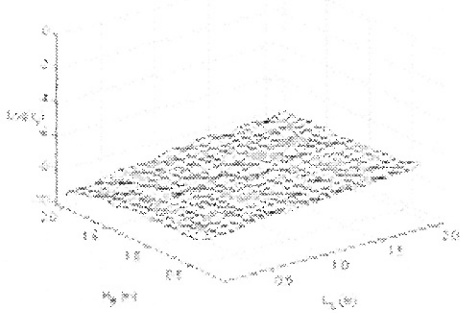


Fig. 12. Plot of  $\xi_y$  vs.  $(H_B, L_S)$  for  $F_C = 0.2$  m,  $\beta = 50\%$ , WG.

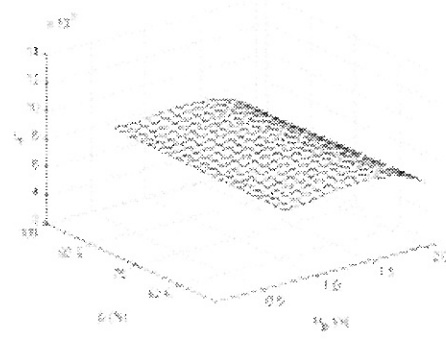


Fig. 16. Plot of  $L_F$  vs.  $(\beta, H_B)$  for  $F_C = 0.5$  m,  $L_S = 1$  m, WG.

### 4.5. Walking Gaits

During our analysis, we concluded that the shape of the plots does not change significantly with the type of gait. As an example, Figures 17 to 20 present the plots of  $\xi_x$  for the *EPHC*, *EPFC*, *BW* and *BEPHC* gaits. Comparing Figures 17 to 20 with Figure 3, it can be seen that the plots are ‘similar’ and that the influence of the different parameters is roughly the same for different types of walking gaits.

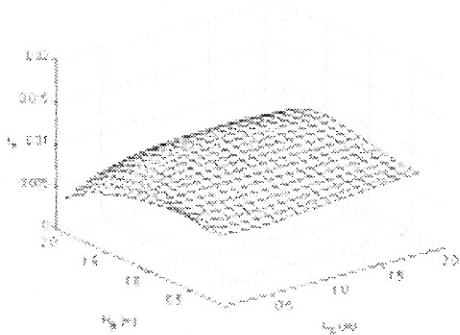


Fig. 13. Plot of  $L_F$  vs.  $(H_B, L_S)$  for  $F_C = 0.2$  m,  $\beta = 50\%$ , WG.

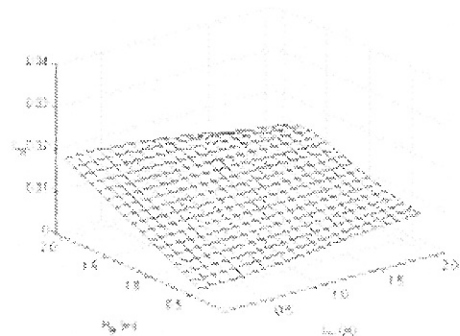


Fig. 14. Plot of  $L_B$  vs.  $(H_B, L_S)$  for  $F_C = 0.2$  m,  $\beta = 50\%$ , WG.

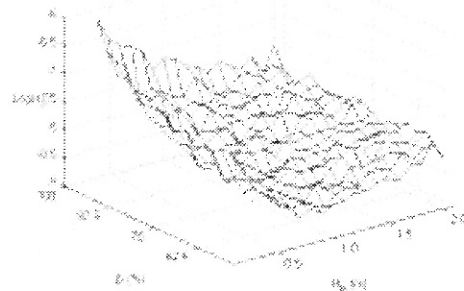


Fig. 17. Plot of  $\xi_x$  vs.  $(\beta, H_B)$  for  $F_C = 0.2$  m,  $L_S = 1$  m, *EPHC*.

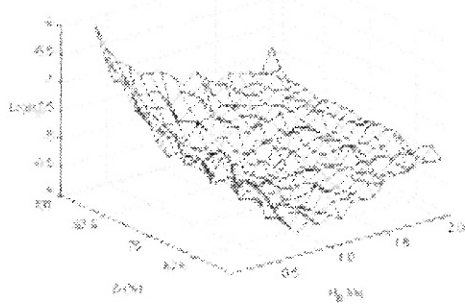


Fig. 18. Plot of  $\xi_{\dot{x}}$  vs.  $(\beta, H_B)$  for  $F_C = 0.2$  m,  $L_S = 1$  m, EPFC.

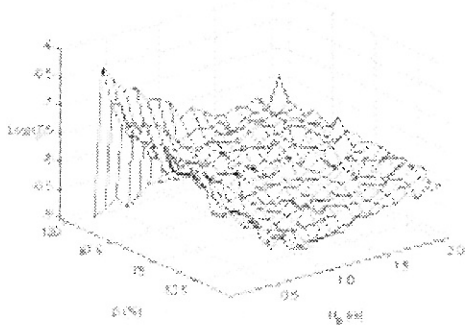


Fig. 19. Plot of  $\xi_{\dot{x}}$  vs.  $(\beta, H_B)$  for  $F_C = 0.2$  m,  $L_S = 1$  m, BW.

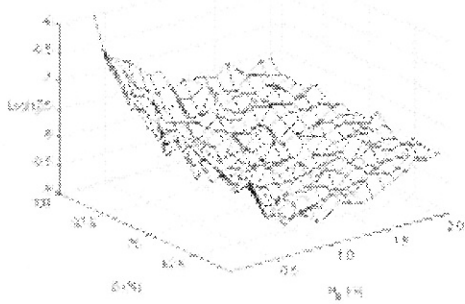


Fig. 20. Plot of  $\xi_{\dot{x}}$  vs.  $(\beta, H_B)$  for  $F_C = 0.2$  m,  $L_S = 1$  m, BEPHC.

## 5. Conclusions

In this paper we have compared various kinematic aspects of multi-legged robot locomotion gaits. By implementing different motion patterns, we estimated how the robot responds to a large variety of locomotion variables such as duty factor, step length, body height, and maximum foot clearance. Two quantitative measures were formulated for analysing the kinematic performance namely a perturbation analysis and a locomobility study. The

perturbation analysis tends to be an elegant although computationally exigent method. Its random characteristics seem to be particularly tailored for examining the role of the different variables on the locomotion process. On the other hand, the locomobility measure captures the geometric amplification between the joints and the foot or body.

While our focus has been on kinematic dexterity, certain aspects of locomotion are not necessarily captured by the proposed measures. Consequently, future work in this area will address the refinement of our models to incorporate the dynamics, as well as exploring non-periodic walking cycles.

## References

- [1] S-M. Song, K.J. Waldron, *Machines that Walk: The Adaptive Walking Vehicle*, The MIT Press, 1989.
- [2] D. J. Manko, *A General Model of Legged Locomotion on Natural Terrain*, Kluwer, Westinghouse Electric Corporation, 1992.
- [3] M. A. Jiménez, P. G. Santos, "Terrain-Adaptive Gait for Walking Machines", *The International Journal of Robotics Research*, Vol. 16, n. 3, pp. 320-339, 1997.
- [4] S.T. Venkataraman, "A Model of Legged Locomotion Gaits", *IEEE International Conference on Robotics and Automation*, Minneapolis, USA, 1996.
- [5] P. Gregorio, M. Ahmadi and M. Buehler, "Design, Control, and Energetics of an Electrically Actuated Legged Robot", *IEEE Transactions on Systems, Man and Cybernetics*, Vol. 27, n. 4, 1997.
- [6] Filipe M. Silva, J. A. Tenreiro Machado, "Energy Analysis During Biped Walking", *IEEE International Conference on Robotics and Automation*, Detroit, Michigan, USA, 1999.
- [7] V. V. Lapshin; "Energy Consumption of a Walking Machine. Model Estimations and Optimization"; *Seventh International Conference on Advanced Robotics*, Sant Feliu de Guixols, Catalonia, Spain, September 20-22, 1995, pp. 420-425
- [8] Filipe M. Silva, J. A. Tenreiro Machado, "Kinematic Analysis of Artificial Biped Locomotion Systems", *1997 IEEE International Conference on Intelligent Engineering Systems*, Budapest, Hungary, September 15-17, 1997.
- [9] David Wettergreen, Chuck Thorpe; "Gait Generation for Legged Robots", *IEEE International Conference On Intelligent Robots and Systems*, Minneapolis, USA, 1992.